ELSEVIER

Inconsistency in the triple layer model description of ionic strength dependent boron adsorption

Sabine Goldberg *

USDA-ARS, George E. Brown Jr. Salinity Laboratory, 450 W. Big Springs Road, Riverside, CA 92507, USA

Abstract

Understanding anion adsorption mechanisms is necessary to allow prediction of anion adsorption behavior. This study was conducted to evaluate the ability of the triple layer model, a chemical surface complexation model, to describe the effect of changes in solution ionic strength (0.01–1.0 M NaCl) and solution pH (3–11) on B adsorption by the iron oxide, goethite, the aluminum oxide, gibbsite, the clay minerals, kaolinite and montmorillonite, and two arid zone soils. Ionic strength dependence of adsorption suggests an inner-sphere adsorption mechanism for goethite, kaolinite, montmorillonite, and the two soils and an outer-sphere adsorption mechanism for gibbsite. The triple layer model, containing an inner-sphere adsorption mechanism, was able to describe B adsorption on goethite, kaolinite, montmorillonite, and the two soils. The model was able to describe B adsorption on gibbsite using an outer-sphere adsorption mechanism. A problematic inconsistency exists in the triple layer model description of ionic strength dependent B adsorption between the type of B surface complex defined in the model and the ionic strength dependence of the model result. That is, postulating an inner-sphere adsorption mechanism in the triple layer model resulted in an ionic strength dependence appropriate for the formation of outer-sphere surface complexes and vice versa. Additional tests of the ability of the triple layer model to describe ionic strength dependent adsorption of additional ions are needed to establish whether the inconsistencies are limited to the B system or are of concern in other triple layer model applications.
Published by Elsevier Inc.

Keywords: Surface complexation modeling; Inner-sphere surface complex; Outer-sphere surface complex; Goethite; Gibbsite; Kaolinite; Montmorillonite; Soil

1. Introduction

Boron is an important element in plant nutrition. Boron toxicity may be a problem in arid areas, while B deficiency is of concern in areas receiving plentiful rainfall [1]. The B solution concentration range between plant deficiency and toxicity is narrow. Plants respond only to the B activity in soil solution and not to B adsorbed on soil minerals [2]. For this reason, understanding of the mechanism of B adsorption on soil materials is essential.

Boric acid is a very weak monobasic acid with a pK_a of 9.2 and a trigonal geometry. It acts as a Lewis acid by accepting a hydroxyl ion to form the borate anion:

$$H_3BO_3 + H_2O \leftrightarrow B(OH)_4^- + H^+. \tag{1}$$
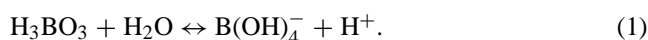
The borate anion has a tetrahedral geometry. Direct experimental evidence for the presence of both trigonal and tetrahedral B on the surface of amorphous Fe oxide was provided by Attenuated Total Reflectance Fourier Transform Infrared (ATR-FTIR) spectroscopy [3,4].

Ligand exchange with surface hydroxyl groups has been invoked as the mechanism of B adsorption on Al and Fe oxide minerals [3,5,6] and clay minerals [7]. Ligand exchange is a mechanism whereby anions become specifically adsorbed onto mineral surfaces forming inner-sphere surface complexes. Inner-sphere complexes contain no water molecules between the adsorbing anion and the surface functional group; while outer-sphere complexes contain at least one

* Fax: +1-951-342-4962.
E-mail address: sgoldberg@ussl.ars.usda.gov.

water molecule between the adsorbing anion and the surface functional group [8]. Adsorbed B formed both inner-sphere and outer-sphere surface complexes on amorphous Fe oxide as observed by ATR-FTIR spectroscopy [4].

The effects of ionic strength on adsorption have been used previously to distinguish between inner-sphere and outer-sphere metal [9] and anion [10] surface complexes on goethite. Selenate showing strong ionic strength dependence in its adsorption behavior was considered weakly bonded as an outer-sphere surface complex, while selenite [10], lead and cadmium [9] showing little ionic strength dependence in their adsorption behavior were considered specifically adsorbed as strong inner-sphere surface complexes. Extended X-ray absorption fine structure (EXAFS) measurements were used to verify the adsorption mechanisms for the selenium species [11]. Using the reasoning of Hayes and co-workers [9–11], Goldberg et al. [12] interpreted their ionic strength dependent B adsorption results to indicate the formation of inner-sphere B surface complexes on goethite, gibbsite, and kaolinite and outer-sphere B surface complexes on montmorillonite and two soils. In a more detailed evaluation of ionic strength effects on ion adsorption, McBride [13] indicated that ions forming inner-sphere surface complexes can show ionic strength dependent adsorption which increases with increasing solution ionic strength. The explanation for this is the principle of mass action. Increased ion adsorption results because of the increased solution activity of the counter ion of the background electrolyte available to compensate the surface charge generated by specific ion adsorption. Reinterpretation of the data of Goldberg et al. [12] using the mass action principle indicates an outer-sphere adsorption mechanism for B on gibbsite and inner-sphere adsorption mechanisms for B on goethite, kaolinite, montmorillonite, and soils.

Surface complexation models such as the constant capacitance model and the triple layer model are chemical models that explicitly define surface complexes and chemical reactions and consider the charge on both the adsorbing anion and the adsorbent solid. The constant capacitance model has been used successfully to describe B adsorption on various Al and Fe oxides, clay minerals, and soils [12,14–17]. The constant capacitance model considers all ions to adsorb specifically forming inner-sphere complexes unaffected by changes in solution ionic strength since the model uses the constant ionic medium Reference State. Solution ionic strength effects can be included by considering activity coefficients for the solution species. The triple layer model can consider both inner-sphere and outer-sphere surface complexes and has been successful in describing ionic strength dependent selenium [10], molybdenum [18], and arsenic [19] adsorption by soil minerals.

For heavy metals, adsorption behavior with ionic strength is a function of the type of background electrolyte [20]. In $NaNO_3$ solutions, Cd, Pb, Co, and Zn adsorption exhibited very little ionic strength dependence. In NaCl solutions, Cd and Cu adsorption decreased strongly with increasing ionic strength. In $NaClO_4$ solutions, Cd, Co, and Ni adsorption increased somewhat with increasing ionic strength. In order to accurately describe heavy metal adsorption in $NaNO_3$ and $NaClO_4$ solutions using the triple layer model, Criscenti and Sverjensky [20] invoked the formation of metal surface complexes that included the background electrolyte anion. Since such surface species were not necessary to describe heavy metal adsorption in NaCl, these authors recommended use of this background electrolyte for metal adsorption studies.

The objective of the present study was to evaluate the ability of the triple layer model to describe the ionic strength effects on B adsorption behavior by oxides, clay minerals, and soils from a background electrolyte of NaCl using the data published previously by Goldberg et al. [12].
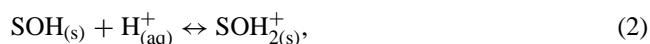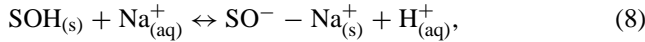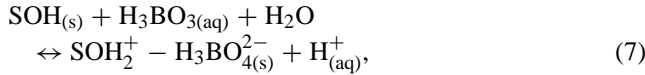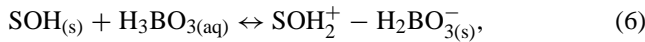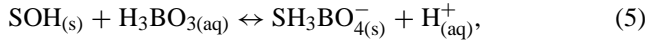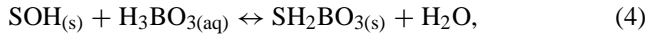
2. Materials and methods

Boron adsorption behavior was studied on goethite (α-FeOOH), gibbsite (α-Al(OH)$_3$), kaolinite (KGa-2, poorly crystallized kaolinite), Na-montmorillonite (SWy-1, Wyoming bentonite), Arlington soil (classified as coarse-loamy, mixed, thermic Haplic Durixeralf), and Bonsall soil (classified as fine, montmorillonitic, thermic Natric Palexeralf). Synthesis methods for the oxide minerals were described by Goldberg et al. [12]. The clay minerals were obtained from the Clay Minerals Society's Source Clays Repository (University of Missouri, Columbia) and used without any pretreatment. The soil samples consisted of the <2-mm fraction of subsurface (25–51 cm) layers of each soil series.

Trace impurities in the oxides and clay minerals and dominant clay minerals in the soils were determined by X-ray diffraction as described in detail by Goldberg et al. [12]. Specific surface areas were determined using N_2 adsorption for oxides and clay minerals and ethylene glycol monoethyl ether (EGME) adsorption for soils (see Goldberg et al. [12] for method details and parameter values).

Experimental details for determining B adsorption envelopes (amount of B adsorbed as a function of solution pH per fixed total B concentration) are given by Goldberg et al. [12]. Samples of adsorbent were added to centrifuge tubes and equilibrated with aliquots of a 5.0 g m^{-3} B solution in NaCl background electrolytes (0.001, 0.01, 0.05, 0.1, and 1 M). The supernatants were analyzed for pH, filtered, and analyzed for B concentration using the colorimetric azomethine-H method described by Bingham [21].

The triple layer model [22] was used to describe B adsorption behavior on the adsorbents. The computer program FITEQL 3.2 [23] was used to fit surface complexation constants to the experimental adsorption data. In the present application of the triple layer model to B adsorption, the following surface complexation reactions were considered:

$$SOH_{(s)} + H^+_{(aq)} \leftrightarrow SOH^+_{2(s)}, \tag{2}$$

$$SOH_{(s)} \leftrightarrow SO^-_{(s)} + H^+_{(aq)}, \tag{3}$$

$$SOH_{(s)} + H_3BO_{3(aq)} \leftrightarrow SH_2BO_{3(s)} + H_2O, \tag{4}$$

$$SOH_{(s)} + H_3BO_{3(aq)} \leftrightarrow SH_3BO_{4(s)}^- + H_{(aq)}^+, \tag{5}$$

$$SOH_{(s)} + H_3BO_{3(aq)} \leftrightarrow SOH_2^+ - H_2BO_{3(s)}^-, \tag{6}$$

$$\begin{aligned} SOH_{(s)} + &H_3BO_{3(aq)} + H_2O \\ &\leftrightarrow SOH_2^+ - H_3BO_{4(s)}^{2-} + H_{(aq)}^+, \end{aligned} \tag{7}$$

$$SOH_{(s)} + Na_{(aq)}^+ \leftrightarrow SO^- - Na_{(s)}^+ + H_{(aq)}^+, \tag{8}$$

$$SOH_{(s)} + H_{(aq)}^+ + Cl_{(aq)}^- \leftrightarrow SOH_2^+ - Cl_{(s)}^-, \tag{9}$$

where SOH represents a reactive surface hydroxyl bound to a metal ion, S (Al or Fe) in the oxide mineral or an aluminol at the clay mineral edge. Both trigonal, Eqs. (4) and (6), and tetrahedral, Eqs. (5) and (7), B surface species were included, consistent with the experimental spectroscopic results [3,4]. Eqs. (4) and (5) describe the formation of inner-sphere B surface complexes since no water is present between the adsorbate B and the surface functional group; while Eqs. (6) and (7) define outer-sphere B surface complex formation since a water molecule is situated between the adsorbate B and the surface functional group. Eqs. (8) and (9) define the outer-sphere surface complexes formed by ions from the background electrolyte. By convention the Na surface complex is considered to be outer-sphere even though no water of hydration is shown between the adsorbed Na ion and the surface functional group. The locations of the various adsorbing ions on the surface are indicated in Fig. 1. While the triple layer model formulation does not expressly assign inner-sphere complexes exclusively to the 0-plane and outer-sphere complexes exclusively to the β-plane, this has been done historically.

Intrinsic equilibrium constants for the surface complexation reactions are:

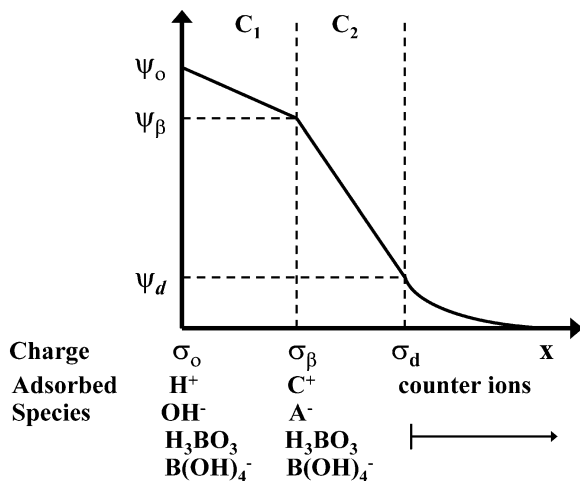$$K_+(\text{int}) = \frac{[SOH_2^+]}{[SOH](H^+)} \exp(F\psi_0/RT), \tag{10}$$

Fig. 1. Placement of ions, surface charges (σ), surface potentials (ψ) and capacitances in the triple layer model (after Westall [29]).

$$K_-(\text{int}) = \frac{[SO^-](H^+)}{[SOH]} \exp(-F\psi_0/RT), \tag{11}$$

$$K_B^{1_{\text{is}}}(\text{int}) = \frac{[SH_2BO_3]}{[SOH](H_3BO_3)}, \tag{12}$$

$$K_{B-}^{2_{\text{is}}}(\text{int}) = \frac{[SH_3BO_4^-](H^+)}{[SOH](H_3BO_3)} \exp(-F\psi_0/RT), \tag{13}$$

$$K_B^{1_{\text{os}}}(\text{int}) = \frac{[SOH_2^+ - H_2BO_3^-]}{[SOH](H_3BO_3)} \exp[F(\psi_0 - \psi_\beta)/RT], \tag{14}$$

$$\begin{aligned} K_{B-}^{2_{\text{os}}}(\text{int}) &= \frac{[SOH_2^+ - H_3BO_4^{2-}](H^+)}{[SOH](H_3BO_3)} \\ &\times \exp[F(\psi_0 - 2\psi_\beta)/RT], \end{aligned} \tag{15}$$

$$\begin{aligned} K_{Na^+}&(\text{int}) \\ &= \frac{[SO^- - Na^+](H^+)}{[SOH](Na^+)} \exp[F(\psi_\beta - \psi_0)/RT], \end{aligned} \tag{16}$$

$$\begin{aligned} K_{Cl^-}&(\text{int}) \\ &= \frac{[SOH_2^+ - Cl^-]}{[SOH](H^+)(Cl^-)} \exp[F(\psi_0 - \psi_\beta)/RT], \end{aligned} \tag{17}$$

where F is the Faraday constant ($C\,mol_c^{-1}$), ψ_0 and ψ_β are surface potentials (V), 0 and β refer to surface planes of adsorption, R is the molar gas constant ($J\,mol^{-1}\,K^{-1}$), T is the absolute temperature (K), square brackets represent concentrations ($mol\,L^{-1}$), and parentheses represent activities. The exponential terms can be considered as solid-phase activity coefficients that correct for charges on the surface complexes.

The total number of reactive surface functional groups is:

$$\begin{aligned} [SOH_T] = {}&[SOH] + [SOH_2^+] + [SO^-] + [SH_2BO_3] \\ &+ [SH_3BO_4^-] + [SOH_2^+ - H_2BO_3^-] \\ &+ [SOH_2^+ - H_3BO_4^{2-}] + [SO^- - Na^+] \\ &+ [SOH_2^+ - Cl^-]. \end{aligned} \tag{18}$$

This parameter is related to the surface site density, N_s (site nm^{-2}):

$$[SOH]_T = \frac{N_s Sa 10^{18}}{N_A}, \tag{19}$$

where S is the surface area ($m^2\,g^{-1}$), a is the solid concentration ($g\,L^{-1}$) and N_A is Avogadro's number.

The charge balance expressions are:

$$\sigma_0 + \sigma_\beta + \sigma_d = 0, \tag{20}$$

$$\begin{aligned} \sigma_0 = {}&[SOH_2^+] + [SOH_2^+ - H_2BO_3^-] + [SOH_2^+ - H_3BO_4^{2-}] \\ &+ [SOH_2^+ - Cl^-] - [SO^-] - [SH_3BO_4^-] \\ &- [SO^- - Na^+], \end{aligned} \tag{21}$$

Table 1
Triple layer model parameters used for the solids

$N_s = 2.31$ sites nm^{-2}
$C_1 = 1.2$ Fm^{-2}
$C_2 = 0.2$ Fm^{-2}

	Goethite	Gibbsite	Kaolinite	Montmorillonite		Bonsall soil	Arlington soil
Inner-sphere B surface complexes							
$\log K_+(int)$	4.3[a]	5.0[a]	5.0[a]	5.0[a]	3.91	4.50	4.25
$\log K_-(int)$	−9.8[a]	−11.2[a]	−11.2[a]	−11.2[a]	−10.83	−10.67	−10.79
$\log K_{Na+}(int)$	−9.3[a]	−8.6[a]	−8.6[a]	−8.6[a]	−10.53	−9.22	[b]
$\log K_{Cl-}(int)$	5.4[a]	7.5[a]	7.5[a]	7.5[a]	4.83	7.44	6.12
$\log K_B(int)$	5.47	7.27	5.25	NC	NC	3.95	NC
$\log K_{B-}(int)$	−1.56	−2.00	−1.97	−1.44	−1.44	−3.20	−3.53
V_Y	78.7	197	127	268	91.8	339	303
Outer-sphere B surface complexes							
$\log K_+(int)$	4.3[a]	5.0[a]	5.0[a]	5.0[a]	5.0[a]	5.0[a]	5.0[a]
$\log K_-(int)$	−9.8[a]	−11.2[a]	−11.2[a]	−11.2[a]	−9.96	−11.2[a]	−10.16
$\log K_{Na+}(int)$	−9.3[a]	−8.6[a]	−8.6[a]	−8.6[a]	−8.30	−8.54	−8.08
$\log K_{Cl-}(int)$	5.4[a]	7.5[a]	7.5[a]	7.5[a]	8.04	7.79	8.18
$\log K_B(int)$	5.87	7.48	5.75	5.77	5.77	4.76	4.45
$\log K_{B-}(int)$	NC	−2.58	NC	−4.65	−4.65	NC	−6.08
V_Y	116	201	554	122	89.2	326	154

NC means no convergence.
[a] Parameters remained fixed and were not optimized.
[b] Parameter was not included.

$$\sigma_\beta = [SO^- - Na^+] - \left[SOH_2^+ - H_2BO_3^-\right]$$
$$- 2\left[SOH_2^+ - H_3BO_4^{2-}\right] - \left[SOH_2^+ - Cl^-\right]. \qquad (22)$$

The surface charge/surface potential relationships are:

$$\sigma_0 = \frac{C_1 Sa}{F}(\psi_0 - \psi_\beta), \qquad (23)$$

$$\sigma_d = \frac{C_2 Sa}{F}(\psi_d - \psi_\beta), \qquad (24)$$

$$\sigma_d = \frac{Sa}{F}(8\varepsilon_0 DRTI)^{1/2}\sinh(F\psi_d/2RT), \qquad (25)$$

where C_1 and C_2 are capacitances, ψ_d is the surface potential at the plane, d, of the diffuse ion swarm, ε_0 is the permittivity of vacuum, D is the dielectric constant of water, and I is the ionic strength.

The surface site density was set at a value of 2.31 sites nm^{-2}, previously recommended by Davis and Kent [24] for natural materials. Numerical values for the intrinsic protonation and dissociation constants and the background electrolyte surface complexation constants were obtained from the literature. For goethite these constants $\log K_+(int) = 4.3$, $\log K_-(int) = -9.8$, $\log K_{Na+}(int) = -9.3$, $\log K_{Cl-}(int) = 5.4$ had been determined previously by Zhang and Sparks [25]. For aluminum oxides, clays, and soils these constants were initially set at: $\log K_+(int) = 5.0$, $\log K_-(int) = -11.2$, $\log K_{Na+}(int) = -8.6$, $\log K_{Cl-}(int) = 7.5$ as obtained by Sprycha [26,27] for γ-Al_2O_3. Two B surface complexation constants were fit simultaneously to the adsorption data at four to five different ionic strengths using either inner-sphere or outer-sphere adsorption mechanisms. For montmorillonite and the soils

it was subsequently necessary to optimize $\log K_{Na+}(int)$ and $\log K_{Cl-}(int)$, followed by $\log K_+(int)$ and $\log K_-(int)$, as well as the boron surface complexation constants. It is preferable and minimizes the number of adjustable parameters to obtain values of protonation–dissociation constants and the surface complexation constants for the background electrolyte experimentally from titration data. These parameters are not generally available for complex natural materials. The capacitances fixed at $C_1 = 1.2$ Fm^{-2} and $C_2 = 0.2$ Fm^{-2} were considered optimum for goethite by Zhang and Sparks [28]. All input parameters and optimized surface complexation constant values are provided in Table 1. The set of surface complexation constants and capacitances were the same parameters used in describing molybdenum [18] and arsenic [19] adsorption by soils and soil minerals. Activity coefficient corrections were included for the solution species using the Davies equation [23].

3. Results and discussion

Boron adsorption as a function of pH and ionic strength for all materials is indicated in Figs. 2–7 (experimental data from Goldberg et al. [12]). Boron adsorption on all materials exhibited the typical parabolic adsorption envelope, where adsorption initially increased as the solution pH increased, an adsorption maximum was reached at intermediate pH, and B adsorption declined as the pH continued to increase. The adsorption maxima were found at pH 7.5–8.5 for goethite (Fig. 2), pH 6–8 for gibbsite (Fig. 3), pH 8–8.5 for kaolinite (Fig. 4), and pH 9–10 for montmorillonite (Fig. 5) and the soils (Figs. 6 and 7). The effect of ionic
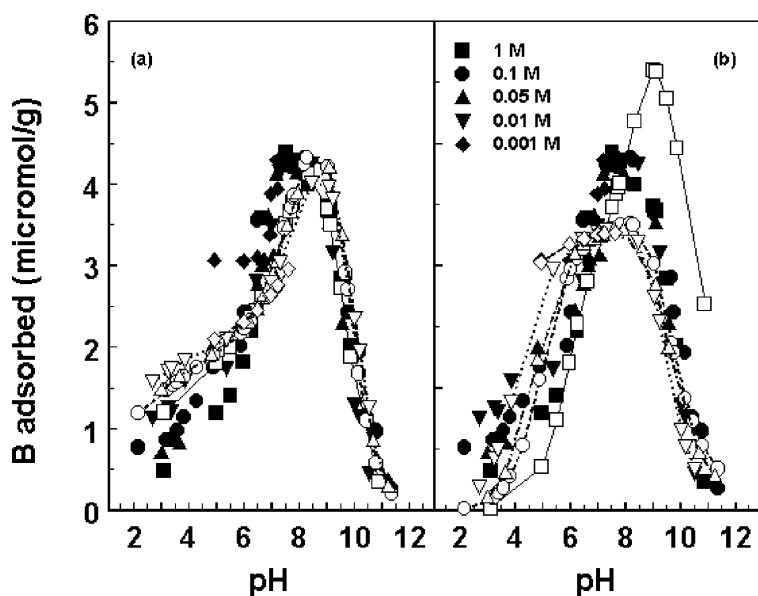
Fig. 2. Boron adsorption on goethite as a function of pH and ionic strength. Filled symbols represent experimental data. Triple layer model results are represented by lines and open symbols: (a) inner-sphere surface complexes: optimizing $\log K_B(\text{int})$ and $\log K_{B^-}(\text{int})$; (b) outer-sphere surface complexes: optimizing $\log K_B(\text{int})$, $\log K_{B^-}(\text{int})$ did not converge. Model parameter values are provided in Table 1.
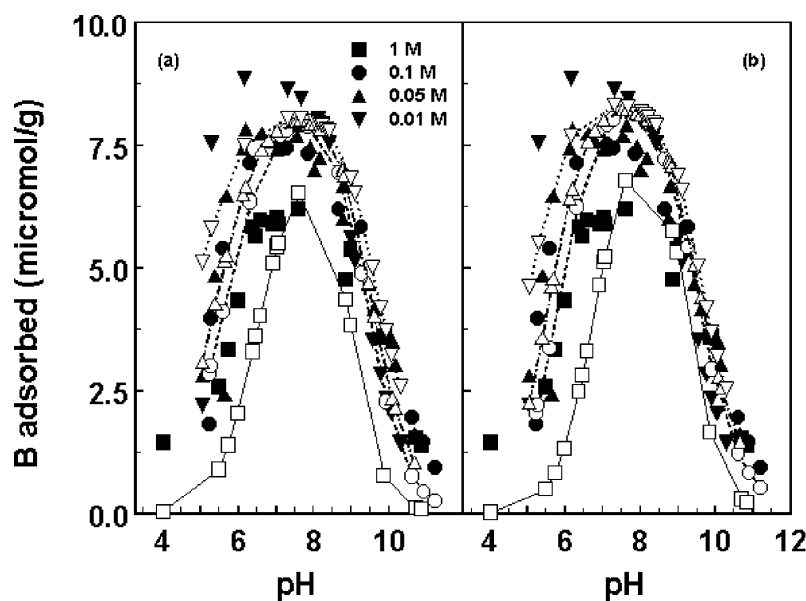

Fig. 3. Boron adsorption on gibbsite as a function of pH and ionic strength. Filled symbols represent experimental data. Triple layer model results are represented by lines and open symbols: (a) inner-sphere surface complexes: optimizing $\log K_B(\text{int})$ and $\log K_{B^-}(\text{int})$; (b) outer-sphere surface complexes: optimizing $\log K_B(\text{int})$ and $\log K_{B^-}(\text{int})$. Model parameter values are provided in Table 1.

strength on B adsorption was investigated for at least two orders of magnitude, from 0.001 or 0.01 to 1.0 M NaCl.

Boron adsorption on goethite (Fig. 2) exhibited very little ionic strength dependence consistent with an inner-sphere adsorption mechanism as had been observed by Goldberg et al. [12]. The triple layer model was able to describe the data using two inner-sphere B surface complexes (Fig. 2a). There was some deviation at lower pHs but the fit at pH above the adsorption maximum was excellent. The trigonal B surface complex was dominant below pH 7. The abil-

ity of the triple layer model to describe B adsorption on goethite using two outer-sphere B surface complexes was not good (Fig. 2b). This is not surprising since this adsorption mechanism contradicts experimental observation. What is surprising is that the model fits show increasing adsorption with increasing ionic strength rather than decreasing adsorption with increasing ionic strength as expected for an outer-sphere adsorption mechanism.

Boron adsorption on gibbsite showed considerable ionic strength dependence consistent with an outer-sphere adsorp-
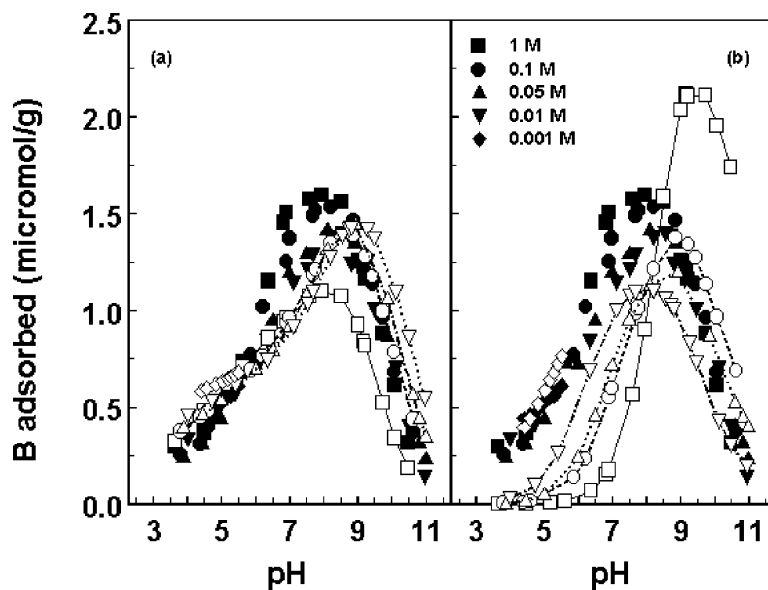
Fig. 4. Boron adsorption on kaolinite as a function of pH and ionic strength. Filled symbols represent experimental data. Triple layer model results are represented by lines and open symbols. (a) Inner-sphere surface complexes: optimizing $\log K_B(\text{int})$ and $\log K_{B-}(\text{int})$; (b) outer-sphere surface complexes: optimizing $\log K_B(\text{int})$, $\log K_{B-}(\text{int})$ did not converge. Model parameter values are provided in Table 1.
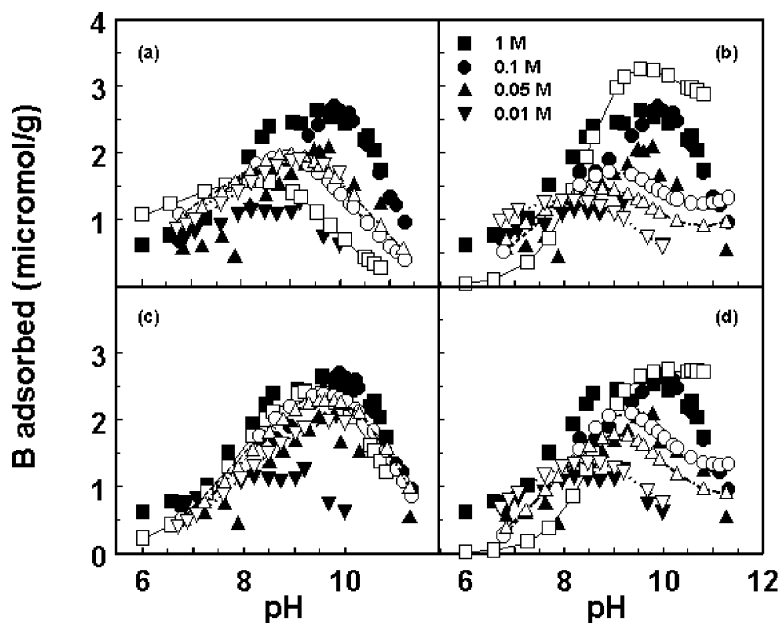

Fig. 5. Boron adsorption on montmorillonite as a function of pH and ionic strength. Filled symbols represent experimental data. Triple layer model results are represented by lines and open symbols. (a) Inner-sphere surface complexes: optimizing $\log K_{B-}(\text{int})$, $\log K_B(\text{int})$ did not converge; (b) outer-sphere surface complexes: optimizing $\log K_B(\text{int})$ and $\log K_{B-}(\text{int})$; (c) inner-sphere surface complexes: optimizing $\log K_{B-}(\text{int})$, $\log K_{Na+}(\text{int})$, $\log K_{Cl-}(\text{int})$, $\log K_+(\text{int})$, and $\log K_-(\text{int})$, $\log K_B(\text{int})$ did not converge; (d) outer-sphere surface complexes: optimizing $\log K_B(\text{int})$, $\log K_{B-}(\text{int})$, $\log K_{Na+}(\text{int})$, $\log K_{Cl-}(\text{int})$, and $\log K_-(\text{int})$, $\log K_+(\text{int})$ was not optimized. Model parameter values are provided in Table 1.

tion mechanism, especially at pHs below the adsorption maximum (Fig. 3). By focusing on the ionic strength dependence of the adsorption maximum, Goldberg et al. [12] had erroneously deduced an inner-sphere adsorption mechanism for this material. While the fits were not quantitative at low pH value, the triple layer model was able to describe the trends in B adsorption with changes in solution ionic strength using two outer-sphere B surface complexation con-

stants (Fig. 3b). Surprisingly, the fits obtained using two inner-sphere B surface complexes were virtually identical (compare Figs. 3a and 3b) with trigonal surface B dominating up to a pH value of 10. What is again surprising, is that the model results for inner-sphere B surface complexes (Fig. 3a), show ionic strength dependent trends in B adsorption that are contradictory to the type of B surface species defined in the model input.
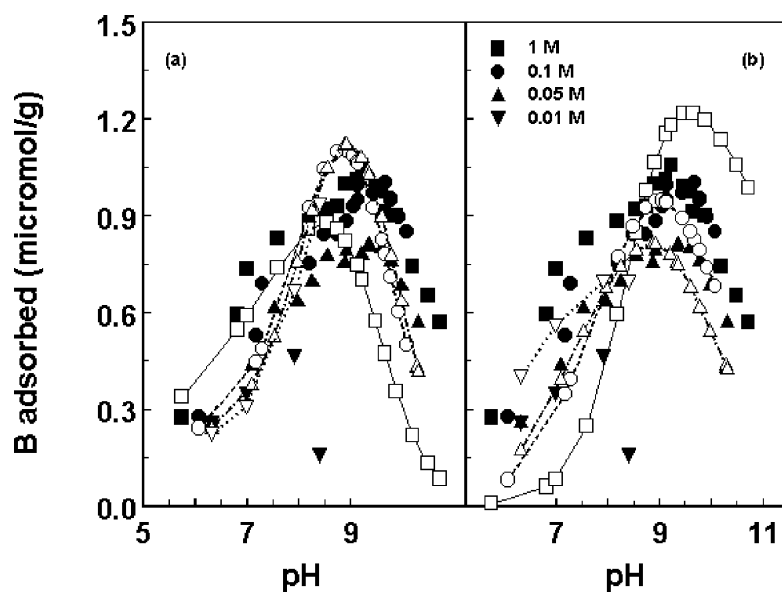
Fig. 6. Boron adsorption on Bonsall soil as a function of pH and ionic strength. Filled symbols represent experimental data. Triple layer model results are represented by lines and open symbols. (a) Inner-sphere surface complexes: optimizing $\log K_B(\text{int})$, $\log K_{B-}(\text{int})$, $\log K_{Na+}(\text{int})$, $\log K_{Cl-}(\text{int})$, $\log K_+(\text{int})$, and $\log K_-(\text{int})$; (b) outer-sphere surface complexes: optimizing $\log K_B(\text{int})$, $\log K_{Na+}(\text{int})$, and $\log K_{Cl-}(\text{int})$, $\log K_+(\text{int})$ and $\log K_-(\text{int})$ were not optimized, $\log K_{B-}(\text{int})$ did not converge. Model parameter values are provided in Table 1.
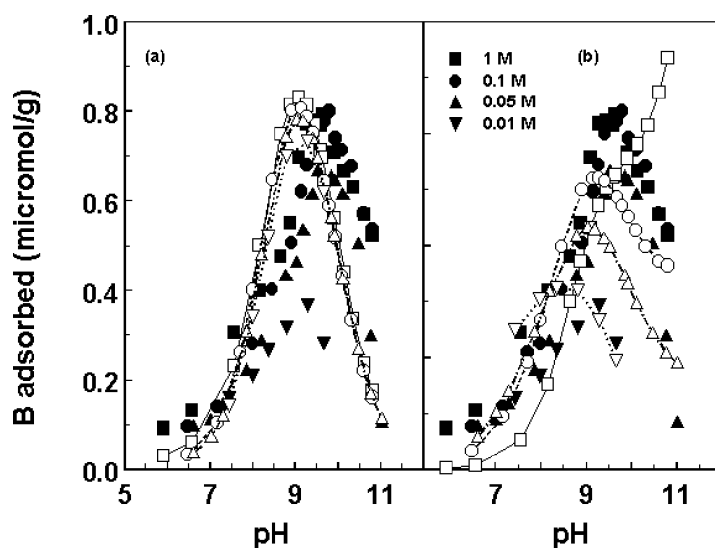

Fig. 7. Boron adsorption on Arlington soil as a function of pH and ionic strength. Filled symbols represent experimental data. Triple layer model results are represented by lines and open symbols. (a) Inner-sphere surface complexes: optimizing $\log K_{B-}(\text{int})$, $\log K_{Cl-}(\text{int})$, $\log K_+(\text{int})$, and $\log K_-(\text{int})$, $\log K_{Na+}(\text{int})$ was not included, $\log K_B(\text{int})$ did not converge; (b) outer-sphere surface complexes: optimizing $\log K_B(\text{int})$, $\log K_{B-}(\text{int})$, $\log K_{Na+}(\text{int})$, $\log K_{Cl-}(\text{int})$, and $\log K_-(\text{int})$, $\log K_+(\text{int})$ was not optimized. Model parameter values are provided in Table 1.

Ionic strength dependence of B adsorption on kaolinite (Fig. 4) was slight as previously observed by Goldberg et al. [12]. Fit of the triple layer model with two inner-sphere B surface complexes reproduced the experimental trends in magnitude of B adsorption; the trigonal B surface complex was dominant at low pH. The model results show increasing adsorption with decreasing ionic strength which is again contradictory to the behavior for inner-sphere adsorption (Fig. 4a). In an exactly analogous contradictory manner, the triple layer fits with two outer-sphere B surface complexes

show increasing adsorption with increasing ionic strength above the B adsorption maximum (Fig. 4b).

Ionic strength dependence of B adsorption on montmorillonite was large and had been interpreted as evidence of an outer-sphere adsorption mechanism by Goldberg et al. [12]. However, this deduction is incorrect. Since adsorption increases with increasing ionic strength, the mechanism of B adsorption is inner-sphere (Fig. 5). The fit of the triple layer model is not good and again exhibits the contradictory result of decreasing adsorption with increasing ionic strength for

inner-sphere B surface complexes (Fig. 5a) and increasing adsorption with increasing ionic strength for outer-sphere B surface complexes (Fig. 5b). Model fits to the data were much improved by additional optimization of the background electrolyte and protonation–dissociation constants (Figs. 5c and 5d). This also resulted in the inner-sphere model fits agreeing with experimental results of increasing B adsorption with increasing ionic strength (Fig. 5c). For the outer-sphere model fit, ionic strength dependence on adsorption behavior still contradicts the type of B surface species defined in the model input and observed experimentally (Fig. 5d).

The fit of the triple layer model to B adsorption on the soils was very poor when optimizing only the B surface complexation constants. Therefore, the fits shown in Figs. 6 and 7 were obtained by optimizing additional constants. As for the montmorillonite, the large ionic strength dependence on adsorption had been erroneously interpreted as evidence of an outer-sphere adsorption mechanism on soils by Goldberg et al. [12]. Boron adsorption on soils increases with increasing ionic strength indicative of an inner-sphere adsorption mechanism (Figs. 6 and 7). The fit of the triple layer model for Bonsall soil, while qualitatively correct, again exhibits the contradictory result of decreasing adsorption with increasing ionic strength for inner-sphere B surface complexes (Fig. 6a) and increasing adsorption with increasing ionic strength for outer-sphere B surface complexes (Fig. 6b). The fit of the triple layer model using two inner-sphere B surface complexes for Arlington soil reproduces the general trends in B adsorption and shows little ionic strength dependence consistent with the experimentally observed inner-sphere adsorption mechanism (Fig. 7a). The fit of the triple layer model using two outer-sphere B surface complexes for Arlington soil again exhibits the contradictory result of increasing adsorption with increasing ionic strength (Fig. 7b).

Previous triple layer model descriptions of cadmium adsorption on silica and alumina in a background electrolyte of $NaClO_4$ showed model trends of decreasing adsorption with increasing ionic strength [20], while the experimental data showed increasing adsorption with increasing ionic strength indicative of an inner-sphere adsorption mechanism. Upon postulating the formation of a Cd–ClO_4 surface complex, the model ionic strength dependence in Cd adsorption reversed to agree with experimental observation. Attempts to consider formation of the sodium-B surface complexes: $SOHNaH_2BO_3$, $SOHNa^+–H_2BO_3^-$, and $SOH_2^+–NaH_3BO_4^-$ in the present triple layer modeling were unsuccessful.

4. Summary

The triple layer model was able to describe B adsorption on Al and Fe oxides, kaolinite, montmorillonite, and two soils simultaneously both as a function of solution pH and solution ionic strength. In the model application to oxides and kaolinite, two adjustable parameters were optimized. While the fit may not be quantitative and requires additional adjustable parameters for montmorillonite and soils, this study shows the potential of the triple layer model. Surface complexation models constitute an advancement over Langmuir and Freundlich isotherm approaches which contain two empirical adjustable parameters but cannot predict changes in adsorption occurring with changes in either solution pH or solution ionic strength.

While the triple layer model is able to describe changes in B adsorption with changing solution ionic strength, a potentially problematic inconsistency exists in its description of this dependence. For several materials, the ionic strength dependence of model B adsorption was contradictory to that observed in the experimental data. More troubling still is the fact that there was inconsistency between the type of B surface complex defined in the model description and the ionic strength dependence of the model result. That is, postulating an inner-sphere adsorption mechanism in the triple layer model resulted in an ionic strength dependence appropriate for the formation of outer-sphere surface complexes and vice versa. Although these inconsistencies were not observed in a prior application of the triple layer model to describe molybdenum adsorption on Fe oxide, Al oxides, kaolinite, montmorillonite, and two soils as a function of solution pH and solution ionic strength [18], additional tests of the ability of the triple layer model to describe ionic strength dependent adsorption of additional anions are needed. Such tests will establish whether the inconsistencies are limited to the B system or are of concern in other triple layer model applications. At present it is recommended that the triple layer model be used only to describe ionic strength dependent B adsorption. For ionic strength independent B adsorption, the constant capacitance model should be used because of its greater simplicity and smaller number of adjustable parameters.

References

[1] R. Keren, F.T. Bingham, Adv. Soil Sci. 1 (1985) 229.
[2] R. Keren, F.T. Bingham, J.D. Rhoades, Soil Sci. Soc. Am. J. 49 (1985) 297.
[3] C. Su, D.L. Suarez, Environ. Sci. Technol. 29 (1995) 302.
[4] D. Peak, G.W. Luther, D.L. Sparks, Geochim. Cosmochim. Acta 67 (2003) 2551.
[5] J.R. Sims, F.T. Bingham, Soil Sci. Soc. Am. Proc. 32 (1968) 364.
[6] M. McPhail, A.L. Page, F.T. Bingham, Soil Sci. Soc. Am. Proc. 36 (1972) 510.
[7] R. Keren, H. Talpaz, Soil Sci. Soc. Am. J. 48 (1984) 555.

[8] G. Sposito, The Surface Chemistry of Soils, Oxford Univ. Press, New York, 1984.

[9] K.F. Hayes, J.O. Leckie, J. Colloid Interface Sci. 115 (1987) 564.

[10] K.F. Hayes, C. Papelis, J.O. Leckie, J. Colloid Interface Sci. 125 (1988) 717.

[11] K.F. Hayes, A.L. Roe, G.E. Brown, K.O. Hodgson, J.O. Leckie, G.A. Parks, Science 238 (1987) 783.

[12] S. Goldberg, H.S. Forster, E.L. Heick, Soil Sci. Soc. Am. J. 57 (1993) 704.

[13] M.B. McBride, Clays Clay Miner. 45 (1997) 598.

[14] S. Goldberg, R.A. Glaubig, Soil Sci. Soc. Am. J. 49 (1985) 1374.

[15] S. Goldberg, R.A. Glaubig, Soil Sci. Soc. Am. J. 50 (1986) 1442.

[16] S. Goldberg, R.A. Glaubig, Soil Sci. Soc. Am. J. 50 (1986) 1173.

[17] S. Goldberg, S.M. Lesch, D.L. Suarez, Soil Sci. Soc. Am. J. 64 (2000) 1356.

[18] S. Goldberg, C. Su, H.S. Forster, in: E.A. Jenne (Ed.), Adsorption of Metals by Geomedia: Variables, Mechanisms, and Model Applications, Academic Press, San Diego, 1998, p. 401.

[19] S. Goldberg, C.T. Johnston, J. Colloid Interface Sci. 234 (2001) 204.

[20] L.J. Criscenti, D.A. Sverjensky, Am. J. Sci. 299 (1999) 828.

[21] F.T. Bingham, in: A.L. Page, et al. (Eds.), Methods of Soil Analysis, second ed., American Society of Agronomy, Madison, 1982, p. 431, part 2.

[22] J.A. Davis, R.O. James, J.O. Leckie, J. Colloid Interface Sci. 63 (1978) 480.

[23] A.L. Herbelin, J.C. Westall, FITEQL: A Computer Program for Determination of Chemical Equilibrium Constants from Experimental Data, Rep. 96-01, Version 3.2, Dep. of Chemistry, Oregon State Univ., Corvallis, 1996.

[24] J.A. Davis, D.B. Kent, Rev. Mineral. 23 (1990) 117.

[25] P. Zhang, D.L. Sparks, Environ. Sci. Technol. 24 (1990) 1848.

[26] R. Sprycha, J. Colloid Interface Sci. 127 (1989) 1.

[27] R. Sprycha, J. Colloid Interface Sci. 127 (1989) 12.

[28] P. Zhang, D.L. Sparks, Soil Sci. Soc. Am. J. 53 (1989) 1028.

[29] J.C. Westall, Am. Chem. Soc. Adv. Chem. Ser. 189 (1980) 33.